Mass Transport in Surface Diffusion of van der Waals Bonded Systems - Boosted by Rotations?

Holly Hedgeland,[*,†,‡] Marco Sacchi,[¶] Pratap Singh,[§] Andrew J. McIntosh,[‡] Andrew P. Jardine,[‡] Gil Alexandrowicz,[‖] David J. Ward,[‡] Stephen J. Jenkins,[⊥] William Allison,[‡] and John Ellis[‡]

†*School of Physical Sciences, The Open University, Walton Hall, Milton Keynes, MK7 6AA, UK*

‡*Cavendish Laboratory, University of Cambridge, JJ Thomson Avenue, Cambridge, CB3 0HE, UK*

¶*Department of Chemistry, University of Surrey, Guildford, GU2 7XH, UK*

§*The Perse School, Cambridge, CB2 8QF, UK*

‖*Department of Chemistry, Technion - Israel Institute of Technology, Haifa 32000, Israel*

⊥*Department of Chemistry, University of Cambridge, Lensfield Road, Cambridge CB2 1EW, UK*

E-mail: holly.hedgeland@open.ac.uk

Abstract

Mass-transport at a surface is a key factor in heterogeneous catalysis. The rate is determined by excitation across a translational barrier and depends on the energy landscape and the coupling to the thermal bath of the surface. Here we use helium spin-echo spectroscopy (HeSE) to track the microscopic motion of benzene adsorbed on Cu(001) at low coverage ($\theta \sim 0.07$ ML). Specifically, our combined experimental and computational data determine both the absolute rate and mechanism of the molecular motion. The observed rate is significantly higher by a factor of 3.0 ± 0.1 than is possible in a conventional, point-particle model and can only be understood by including additional molecular (rotational) coordinates. We argue that the effect can be described as an entropic contribution that enhances the population of molecules in the transition state. The process is generally relevant to molecular systems and illustrates the importance of the pre-exponential factor alongside the activation barrier in studies of surface kinetics.

Graphical TOC Entry

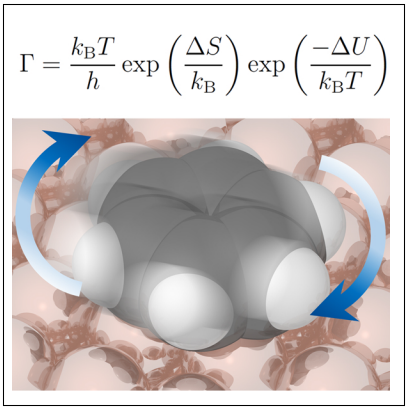

Surface diffusion leads to mass-transport on a surface and, in thermal equilibrium, it involves the motion of an adsorbate through an energy landscape containing one or more energy barriers.[1] In describing the motion of atoms and simple rigid molecules it is conventional to treat them within a 'point' approximation; however, molecular degrees of freedom are known to affect the dynamics in a number of ways. For example, in the diffusion of Pyrrole (C_4H_4NH), zero-point motion in internal coordinates of the molecule gives rise to enhanced diffusion barriers.[2] In larger molecules still, studies using scanning probe microscopy[3,4] and helium spin-echo spectroscopy[5] have shown that there is an intimate connection between rotational transitions of a molecule and its translational motion. Rotation affects translation through coupling where quasi-static rotation steers the molecule towards the lowest barrier of the energy landscape, or where the barrier is reached by a series of frustrated rotations resulting in a favourable geometry on approach to the transition state.[6] Here we demonstrate an entirely different mechanism whereby the internal coordinates of a molecule boost the rate at which the barrier is crossed. In this picture, the entropy of the adsorbed molecule in the transition state is crucial in determining the pre-exponential factor for the rate.

In many cases, the entropy of an adsorbed molecule is higher than expected[7] and entropic effects have been suggested as the cause of the increased rate of diffusion in the case of CO dimers and chains.[8] More recent work has highlighted the importance of accurate estimation of the surface entropy in systems near desorption.[9,10] Yet there are few cases in which experimental rates are determined sufficiently accurately to distinguish the exponential factor from effects arising from the entropic term in the pre-exponential.

Another critical question, highlighted in,[9] is the extent to which the experimental data can be predicted using first-principle calculations. Even a small molecule such as benzene remains challenging to density functional theory (DFT) due to the van der Waals nature of the bonding with many metallic surfaces.[11] Whilst van der Waals (vdW) functionals[12,13] and semi-empirical correction schemes[14] are growing in application and accuracy, their use is still not ubiquitous. In the case of adsorption of small aromatics, calculations are often

benchmarked on close-packed facets of metal surfaces, with far fewer studies using surfaces with more open structures; for C_6H_6 adsorbed to the Cu(001), two previous studies of the system have been published, both carried out prior to the advent of the current generation of van der Waals schemes.[15,16]

In the present work, we have studied benzene adsorbed upon the coinage metal surface Cu(001). Our analysis indicates an unexpected diffusion mechanism where rotations enhance the translational motion. In particular, we show that the rate for translational diffusion is significantly greater than that of a point-like particle moving in the landscape. This remarkable observation cannot be understood in terms of quasi-static steering. Instead, we propose a thermodynamic mechanism whereby an entropic contribution adds to the absolute rate.

Helium atom scattering provides known sensitivity to organic adsorbates[2,5,17] and here we determine the benzene-substrate energy landscape from Helium Spin-Echo (HeSE) measurements of the thermal motion of adsorbed benzene. The principle of the technique[18] is illustrated in figure 1(a), whilst a detailed description has been given elsewhere.[19,20] In brief, helium atoms scatter from mobile adsorbates on the surface, providing a measurement of the correlation in their positions with time. An individual HeSE measurement gives the time decay of the spatial Fourier Transform of the surface correlation function for a particular momentum transfer, $\Delta\mathbf{K}$, through the intermediate scattering function (ISF), $I(\Delta\mathbf{K}, t)$,[21,22] which represents the rate of 'dephasing' of the adsorbate positions, with time, t, in the picosecond range, and over a periodic length-scale $2\pi/\Delta\mathbf{K}$. A typical result showing the behavior of the normalized polarization, P/P_o, which is proportional to the ISF, is shown in figure 1(b). By examining the variation of the ISF across a range of experimental conditions (varying temperature, scattering direction, and $\Delta\mathbf{K}$), we build up a detailed, atomistic picture of motion on the surface.[20]

A decay with increasing time, t, in $I(\Delta\mathbf{K}, t)$ indicates a mobile adsorbate species, with a loss in surface correlation due to diffusion. In order to find the surface dephasing rate, α, we

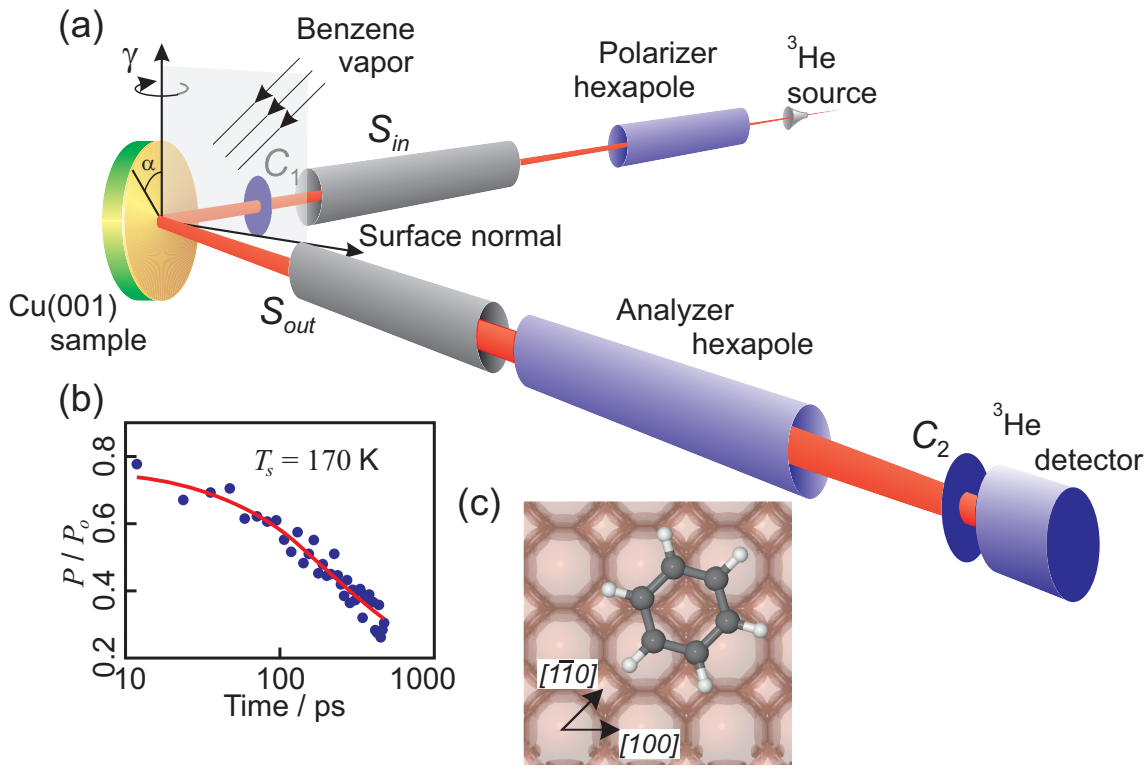

Figure 1: (a) illustration of the experimental arrangement. The beam of ^{3}He is created in the source (top right), then polarized, using a hexapole magnet, focussed and collimated before interacting with the Cu(001) sample. After scattering, the polarization state of the beam is analyzed in another hexapole before the beam enters the detector (bottom right). The polarization state is determined as a function of the spin-echo time, which is determined by the current in the two spin-echo solenoids, S_{in} and S_{out} (see *Jardine et al.*[18] for details). (b) shows typical data at a surface temperature of 170 K. The polarization, P/P_o is plotted as a function of the spin-echo time, for $\Delta\mathbf{K} = 1.8$ Å^{-1}. Measurements are shown as blue circles and the red line is a single exponential function. The logarithmic time-axis shows that a single exponential (solid line) provides a good description of the data throughout the range shown. (c) the surface geometry showing the high symmetry directions of the Cu(001) surface, as used in the measurements, and the calculated adsorption geometry with the centre of the molecule located at a four-fold site.

assume a single exponential decay of $ae^{-\alpha t} + c$ with static level, $c(\Delta\mathbf{K})$ (the standard form for diffusion on a Bravais lattice[18]). The dephasing rate, α, is determined using a Bayesian method[23] (further details in the Supporting Information).

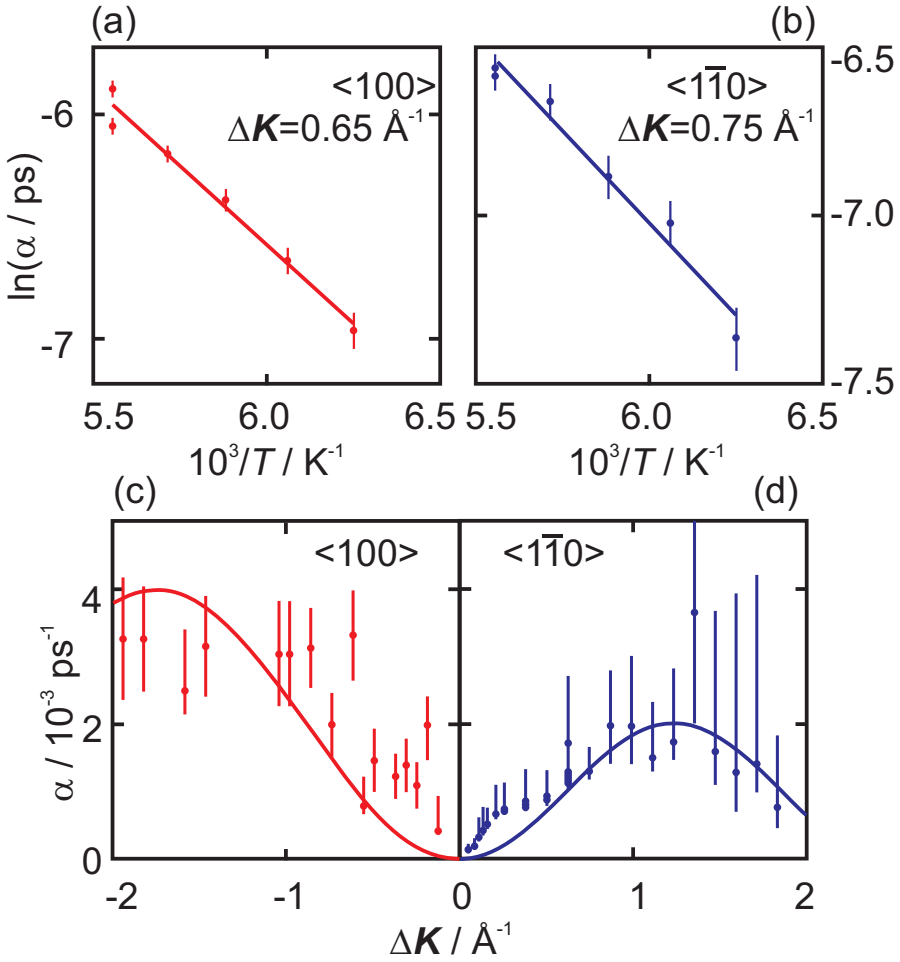

Figure 2: Dephasing rates, $\alpha(\Delta\mathbf{K}, T)$, determined from the measurements of $I(\Delta\mathbf{K}, t)$. (a) and (b) show the temperature dependence of α as Arrenhius plots, along the <100> and <1$\bar{1}$0> directions respectively, for values of $\Delta\mathbf{K}$ indicated. The lines are fits to the Arrenhius form giving an effective activation energy (see text). (c) and (d) show the $\Delta\mathbf{K}$ dependence of the dephasing rate, α, measured at a surface temperature of 170 K. The solid lines correspond to the analytic model for ideal jump-diffusion on a square lattice of four-fold sites with the diffusion barrier located at the bridge-sites.

The temperature dependence of the dephasing rate was measured between 160–180 K at $\Delta\mathbf{K} = 0.65$ Å^{-1} along <100> and 0.75 Å^{-1} along <1$\bar{1}$0> for a coverage of 0.07 ML. The data is presented as points in the Arrhenius plots shown in figures 2(a) and (b), respectively. An effective activation energy for benzene diffusion on the surface can be obtained from the slope

of these graphs. In the <100> direction we find an activation energy of 120.7±7.6 meV and along <1$\bar{1}$0>, 91.0±9.1 meV. The two values correspond to different values of momentum transfer and the small difference between them is not unexpected. Better values for the adiabatic energy barrier are discussed below, in the context of a detailed and quantitative analysis of the complete data-set.

The dependence of the dephasing rate on the momentum transfer, $\Delta\mathbf{K}$, was also measured at a fixed surface temperature of 170 K. Figure 2(c) and (d) show results obtained in the <100> and <1$\bar{1}$0> directions respectively. The data shows that the motion broadly corresponds to hopping between four-fold hollow sites via a barrier at the bridge site, as illustrated by the solid lines in figures 2(c) and (d). The lines come from an analytic model for hopping[24] with a rate scaled to match the data. Agreement between the model and the data, both in the overall $\Delta\mathbf{K}$ dependence and in the relative magnitude of the <100> and <1$\bar{1}$0> directions is a strong indication that the motion is dominated by hopping between four-fold sites.

At low momentum transfers, $< 0.5\text{Å}^{-1}$, the experimental data lies above the analytic model and shows a local maximum, which is particularly evident in the <1$\bar{1}$0> direction. Such features are a signature of repulsive interactions between neighbouring benzene molecules and have been seen with other aromatic adsorbates.[2]

Having established the main features of the diffusion mechanism and approximate values for the diffusion barrier, we now turn to a determination of the absolute rate of the processes involved. For this purpose we perform a more detailed analysis of the data using molecular dynamics (MD), within a Langevin model. The resulting motion is combined with kinematic scattering calculations to generate data that can be compared to experiment.[25] The method was initially developed for alkali metal diffusion and has also been used with considerable success in the interpretation of data from benzene/graphite[26] and other small molecular systems.[2,27–29] In the first instance, we treat the molecule as a point mass. Later we show that it is necessary to refine the treatment and consider the adsorbate as an extended molecular

system.

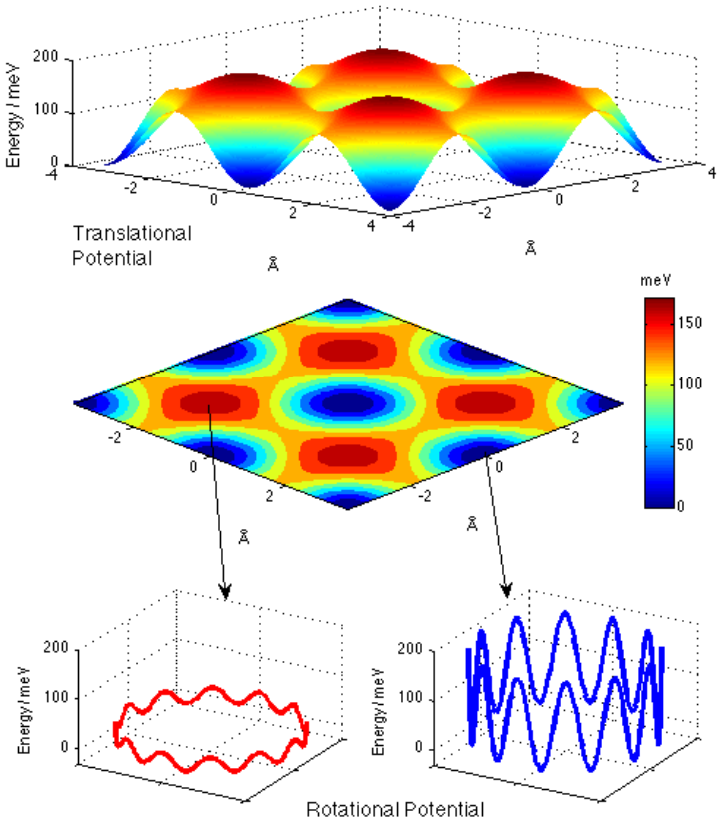

Figure 3: The energy landscapes used in the Langevin simulations. The upper panels show four unit cells of the translational potential energy surface (PES) with a four-fold hollow site located at the centre (see text). The color map extends from the lowest energy (hollow site) to the highest transition-state (top site, 172 meV), with the most favorable transition across the bridge site at 122 meV. The lower panels show the form used for the rotational motion: on the left (red line) is the potential assumed at the bridge and top transition-states; on the right (blue line) is the form assumed at the adsorption site. A molecule on the adsorption site experiences a rotational barrier of 180 meV whilst one at a bridge or top site has a lower rotational barrier of 30 meV.

The adiabatic potential energy surface (PES) is that used previously for (001) surfaces.[25]

The functional form is illustrated in the upper panels of figure 3 and is detailed in full in the Supporting Information. The two free parameters are the relative energies of the top and bridge sites above the hollow adsorption site, E_T and E_B, respectively. These are optimized in the simulations using the experimentally measured temperature dependence and the top to bridge site energy ratio, which affects the relative magnitude of dephasing rates measured along the two principal crystallographic directions. We now vary the one remaining parameter in the Langevin simulation, namely the friction, η, in an attempt to match the magnitude of the dephasing rates in the simulation and experiment. The friction affects the rates in a complex way that can be understood from Kramers' turnover theory.[30] At low values of the friction, the rate increases with increasing friction as more frequent changes in energy lead to more jump attempts; for high friction, the molecule performs Brownian motion over the transition state and so the rate decreases as the friction increases, a result that is also seen in the case of memory friction.[31] Figure 4(a) and (b) show the calculated dephasing rate, α, as a function of the friction, η, at values of $\mathbf{\Delta K}$ that correspond to the maximum in the $\alpha(\mathbf{\Delta K})$ dependence along the $<100>$ and $<1\bar{1}0>$ directions, respectively. The dashed curves correspond to the motion of a point mass, equal to that of the benzene molecule, diffusing in the optimized energy landscape, while the horizontal bar indicates the experimental dephasing rate. We note that, for a point-particle (dashed curve), all values of the friction, η, result in rates that are less than the experiment. It follows that a point-like adsorbate would diffuse too slowly to generate the results we observe. Expressed in an alternative way, we conclude that the molecule has an anomalously large diffusion rate.

The model based on a point-like particle underestimates the magnitude of the dephasing rate, which corresponds to an underestimation of the hopping rate for diffusion. In transition state theory the hopping rate is typically expressed as

$$\Gamma = \frac{k_{\mathrm{B}}T}{h} \exp\left(\frac{-\Delta F}{k_{\mathrm{B}}T}\right),$$

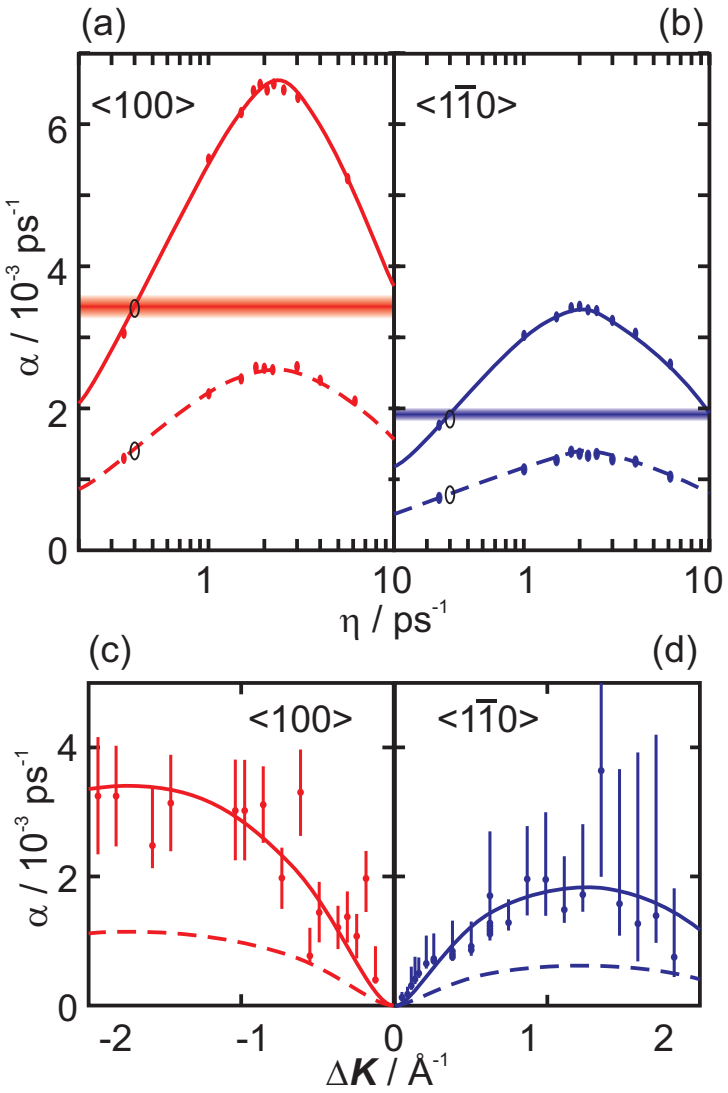

Figure 4: Dephasing rates with (solid) and without (dashed) rotational motion. (a) and (b) show, respectively, calculated dephasing rates in the <100> direction, red points and curves, and in the <1$\bar{1}$0> direction, blue points and curves. In both cases the points are calculated values while the curves are smooth interpolations. The calculation is made at values of $\Delta\mathbf{K}$ corresponding to the maximum rates (see panels (c) and (d), below). The dashed lines correspond to a simulation with translation but no rotation, while the solid lines show the results when rotation is included fully. The horizontal bars represent the experimental dephasing rates, where the width is an estimate of the experimental uncertainty. (c) and (d) show the dephasing rates obtained from simulations, after optimization of the parameters, alongside the experimental results (solid circles with error bars). As before, the dashed and solid lines correspond respectively to simulations with translation only and with translation+rotation. The effect of rotational motion is evident throughout from the increase in dephasing rates with both curves having $\eta = 0.4$ ps^{-1}, the value highlighted in panels (a) and (b).

where $\Delta F = \Delta U - T\Delta S$ is the free energy of activation. The rate is determined both by an Arrenhius factor, $\exp -\Delta U/k_{\mathrm{B}}T$, and the prefactor, which depends on the entropy difference between the adsorption site and the transition state,

$$\Gamma = \frac{k_{\mathrm{B}}T}{h} \exp\left(\frac{\Delta S}{k_{\mathrm{B}}}\right) \exp\left(\frac{-\Delta U}{k_{\mathrm{B}}T}\right).$$

In the case of a molecule like benzene, there are additional degrees of freedom offering an entropic mechanism to increase the hopping rate over that of a point particle. We approach a more realistic modelling of molecular diffusion by introducing an additional dynamical variable within the Langevin simulation. We have chosen to include simple rotational motion about the six-fold molecular axis, using a sinusoidal potential consistent with the six-fold symmetry of benzene on the four-fold Cu(001) surface (see figure 3 and Supporting Information). The details of the mechanism are not essential to our argument since our aim is simply to demonstrate that one or more molecular coordinates results in an enhancement of the diffusion rate. In order to create the entropic difference, we have a barrier to rotation that varies with translational position within the unit cell, as illustrated in the lower panels of figure 3. Specifically, to generate the necessary entropic enhancement to the diffusion rate, the rotational barrier must be greater at the adsorption site than at the transition state.

The complete data-set was re-analysed, taking into account the temperature dependence of the rates and the full $\alpha(\Delta\mathbf{K})$ dependence. We find excellent agreement between the measurement and the simulation if the barrier to rotation decreases from 180 meV at the hollow adsorption site to 30 meV at the bridge and top sites, coupled with the previously described translational PES of $E_T = 172$ meV and $E_B = 122$ meV. We obtain a friction coefficient, η of 0.4 ps^{-1}; the same friction parameter is used for both the translational coordinates and rotational degrees of freedom. Figure 4(c) and (d) show the simulations (solid lines) and measured results (data points) for $\alpha(\Delta\mathbf{K})$ along the <100> and <1$\bar{1}$0> directions respectively. There is good agreement throughout the range of $\Delta\mathbf{K}$ measured. In particular, the absolute

dephasing rates are now in excellent agreement with the data, unlike the analytical model of figure 2 where the rate scaling was arbitrary. The transformation achieved by including a rotational coordinate is evident from the solid lines, showing translation and rotation, in comparison with the dotted lines for a purely translational simulation (figures 4(c), (d)).

Rotation increases the dephasing rates by a factor of approximately 3. In this classical simulation, similar results can be achieved with larger barriers to rotational motion provided the values at the adsorption site and the transition states remain in the same ratio. Lower energies affect the activation energy seen in an Arrhenius plot and hence the values given here are a lower limit. In contrast, for the translational PES, changes of the order of 10 meV in either direction will have a noticeable impact on the simulated temperature dependence. A comparison of rates as a function of Langevin friction is shown in figures 4(a), (b) for a single $\Delta\mathbf{K}$ value. Whilst this clearly allows the Kramers' turnover to be seen, it must be remembered that the shape (curvature) of the momentum transfer dependency will also vary with η (as the number of multiple jumps is affected) and hence the full $\Delta\mathbf{K}$ range needs to be considered when determining the optimum friction coefficient.

We have shown that, in order to understand the translational diffusion of benzene/Cu(001) at a quantitative level, we need to take into account the higher dimensionality of the molecular species and treat it as an extended entity with additional dynamical variables with the entropic effect of these molecular coordinates enhancing the diffusion rate. In our modelling, we created a potential allocated to one specific mode, that of rotation about an axis perpendicular to the surface, through the centre of mass. The rotational potential that we employed (figure 3) decreases in energy by a factor of six between the hollow and top/bridge sites, increasing the density of states at the transition point over the bridge site and hence the probability of its occupation. The choice of the rotational mode is illustrative of the required effect on the density of states at the transition state, rather than definitive. In reality, a larger number of modes may be involved since even a small molecule such as benzene has 34 internal modes available. Smaller changes in vibrational energy levels distributed over

a larger number of modes would result in the same overall change in the density of states at the transition state and consequently the dephasing rates observed in the ISF. However, these modes are typically too high in energy to be activated at the 170 K of our experiment [32] and rotations remain the likely candidate to dominate the entropic effect.

Since the benzene interaction with Cu(001) is dominated by van der Waals interactions, the system also makes an ideal benchmark for vdW DFT calculations. We carried out calculations within CASTEP [33] (for details, see Experimental Methods) and the calculated total energies for the high symmetry surface sites are given in a table in the Supporting Information as a function of the angle of rotation of the molecule about an axis perpendicular to the surface through the centre of mass.

DFT predicts an order of stability for the high symmetry sites (hollow > bridge > top) that is consistent with the experimental data. If we compare the vdW DFT energy barriers of 351 meV over the bridge and 500 meV over the top site with the experimental values, we find that the dispersion-corrected DFT tends to overestimate the corrugation of the benzene/Cu(001) PES, but correctly predicts that the activation barriers for this system to be higher than for the similar systems of cyclopentadienyl/Cu(111) [28] and thiophene/Cu(111). [29] DFT is not only able to predict the preferential pathway for diffusion (hollow to hollow through bridge), but even to estimate with a fair amount of accuracy the ratio between the diffusion barriers on different sites: $E_{top}/\mathrm{E}_{bridge} = 1.42$ for the DFT calculations, compared to an experimental value of 1.41 ($E_{top} = 172$ meV; $E_{bridge} = 122$ meV). Rotational barriers are smaller than those required to give the entropic enhancement required by the analysis above but, given the level of variation between the calculated translational potential and the measured activation energies, we would have little confidence in using the calculations to attempt a detailed assignation of the entropic effects. There is some evidence in the calculated values (see SI) that the rotational potential at the adsorption site has a narrower minimum than elsewhere. Changes in the curvature of the rotational potential offer an additional mechanism that could give an entropic enhancement to the rate of barrier crossing.

If rotational states at the adsorption site were more widely spaced than at the transition state (bridge-site) then the two partition functions would indicate a similar enhancement to the rate of barrier crossing to that in our analysis above.

The difference between the experimental and theoretical values of the translational barrier is greater than in previous studies of adsorbed aromatics,[2,29] which may be due to the fact that the earlier calculations relate to the Cu(111) surface, rather than Cu(001). We are aware that the majority of previous studies using benzene adsorption to benchmark vdW corrections have also used only a (111) surface.[34,35] Our results here might suggest that screening effects could be playing a greater role in the bonding on the more open surface, motivating further inclusion of many-body effects as approached in.[36,37]

In summary, our study of benzene/Cu(001) highlights the importance of entropic effects on the dynamics of adsorbed aromatics as well as the necessity to explore the full potential energy landscape. We highlight the role played by the additional degrees of freedom of molecular adsorbates in the resultant surface dynamics, specifically in altering the density of states at the transition state along the diffusion pathway, and hence affecting the pre-factor of the activated diffusion mechanism. Our DFT calculations show agreement with the diffusion pathway but illustrate that there remain areas where the current approaches have a limited ability to provide quantitative predictions. Experimental benchmark data from surface systems such as benzene/Cu(001) therefore remains of broad interest and challenge to the theoretical community as we seek to develop modelling to chemical accuracy across a wider range of applications.

Experimental methods

A single crystal Cu(001) sample was mounted in the scattering chamber with a base pressure of 1×10^{-10} mbar and was cleaned by repeated cycles of Ar^+ sputtering (800 eV, 10 μA, 10 minutes at 300 K) and annealing (800 K, 30 s). The surface quality was monitored through

the sample's reflectivity to the helium beam and the shape and intensity of the helium scattering specular peak. Benzene (>99.9% purity, Aldrich), previously cleaned by freeze-thaw cycles, was deposited on the surface by backfilling the chamber and monitoring the drop in the specularly reflected helium beam during adsorption. Using a cross-sectional area per benzene molecule from previous diffraction data[38] results in absolute coverage estimated at 0.07 monolayers (ML), achievable with a reproducibility of better than 5%.

DFT calculations were performed using CASTEP[33] and employed the Tkatchenko-Scheffler (TS) dispersion force correction method[39] where the Kohn-Sham energy of the system, calculated with the PBE functional, is corrected by adding a pairwise interatomic energy[40] and the C_6 coefficients are calculated from the ground-state electron density. The Cu(001) surface was modeled by a seven-layer slab where the top three layers were unconstrained. We used electronic and convergence parameters similar to those in *Sacchi et al.*:[41] 300 eV energy cut-off, a (4×4×1) k-point grid, 0.05 eV/Å force tolerance.

Acknowledgement

The authors are grateful for the support of the Leverhulme Trust (HH) and the Royal Society (MS). Via our membership of the UK's HEC Materials Chemistry Consortium, which is funded by EPSRC (EP/L000202), this work used the ARCHER UK National Supercomputing Service.

Supporting Information Available

The Supporting Information contains: further details of the Bayesian method, the Langevin MD simulations and the DFT calculations, including a table of the calculated adsorption energies. This material is available free of charge via the Internet at `http://pubs.acs.org/`.

References

(1) Ala-Nissila, T.; Ferrando, R.; Ying, S. C. Collective and Single Particle Diffusion on Surfaces. *Advances in Physics* **2002**, *51*, 949–1078.

(2) Lechner, B. A. J.; Hedgeland, H.; Ellis, J.; Allison, W.; Sacchi, M.; Jenkins, S. J.; Hinch, B. J. Quantum Influences in the Diffusive Motion of Pyrrole on Cu (111). *Angew. Chem. Int. Ed.* **2013**, *125*, 5189–5192.

(3) Cheng, Z.; Chu, E. S.; Sun, D.; Kim, D.; Zhu, Y.; Luo, M.; Pawin, G.; Wong, K. L.; Kwon, K.-Y.; Carp, R. et al. Tunability in Polyatomic Molecule Diffusion through Tunneling versus Pacing. *J. Am. Chem. Soc.* **2010**, *132*, 13578–13581, PMID: 20831159.

(4) Antczak, G.; Kamiński, W.; Sabik, A.; Zaum, C.; Morgenstern, K. Complex Surface Diffusion Mechanisms of Cobalt Phthalocyanine Molecules on Ag(100). *J. Am. Chem. Soc.* **2015**, *137*, 14920–14929, PMID: 26584143.

(5) Rotter, P.; Lechner, B. A. J.; Morherr, A.; Chisnall, D. M.; Ward, D. J.; Jardine, A. P.; Ellis, J.; Allison, W.; Eckhardt, B.; Witte, G. Coupling between Diffusion and Orientation of Pentacene Molecules on an Organic Surface. *Nature Mater.* **2016**, *15*, 397–400.

(6) Backus, E. H. G.; Eichler, A.; Kleyn, A. W.; Bonn, M. Real-Time Observation of Molecular Motion on a Surface. *Science* **2005**, *310*, 1790–1793.

(7) Weaver, J. F. Entropies of Adsorbed Molecules Exceed Expectations. *Science* **2013**, *339*, 39–40.

(8) Briner, B. G.; Doering, M.; Rust, H.-P.; Bradshaw, A. M. Microscopic Molecular Diffusion Enhanced by Adsorbate Interactions. *Science* **1997**, *278*, 257–260.

(9) Campbell, C. T.; Sellers, J. R. V. The Entropies of Adsorbed Molecules. *J. Am. Chem. Soc.* **2012**, *134*, 18109–18115, PMID: 23033909.

(10) Campbell, C. T.; Arnadottir, L.; Sellers, J. R. V. Kinetic Prefactors of Reactions on Solid Surface. *Z. Phys. Chem.* **2013**, *227*, 1435–1454.

(11) Jenkins, S. J. Aromatic Adsorption on Metals via First-Principles Density Functional Theory. *Proc. R. Soc. A* **2009**, *465*, 2949–2976.

(12) Dion, M.; Rydberg, H.; Schröder, E.; Langreth, D. C.; Lundqvist, B. I. Van der Waals Density Functional for General Geometries. *Phys. Rev. Lett.* **2004**, *92*, 246401.

(13) Klimeš, J.; Bowler, D. R.; Michaelides, A. Chemical Accuracy for the van der Waals Density Functional. *J. Phys.: Condens. Matter* **2010**, *22*, 022201.

(14) McNellis, E. R.; Meyer, J.; Reuter, K. Azobenzene at Coinage Metal Surfaces: Role of Dispersive van der Waals Interactions. *Phys. Rev. B* **2009**, *80*, 205414.

(15) Chen, W.-K.; Cao, M.-J.; Liu, S.-H.; Xu, Y.; Li, J.-Q. On the Coverage-Dependent Orientation of Benzene Adsorbed on Cu(100): A Density Functional Theory Study. *Chem. Phys. Lett.* **2005**, *407*, 414 – 418.

(16) Lorente, N.; Hedouin, M. F. G.; Palmer, R. E.; Persson, M. Chemisorption of Benzene and STM Dehydrogenation Products on Cu(100). *Phys. Rev. B* **2003**, *68*, 155401.

(17) Becker, J. S.; Brown, R. D.; Killelea, D. R.; Yuan, H.; Sibener, S. J. Comparative Surface Dynamics of Amorphous and Semicrystalline Polymer Films. *Proc. Natl. Acad. Sci. U. S. A.* **2011**, *108*, 977–982.

(18) Jardine, A. P.; Alexandrowicz, G.; Hedgeland, H.; Allison, W.; Ellis, J. Studying the Microscopic Nature of Diffusion with Helium-3 Spin-Echo. *Phys. Chem. Chem. Phys.* **2009**, *11*, 3355–74.

(19) Mezei, F. Neutron Spin Echo: A New Concept in Polarized Thermal Neutron Techniques. *Z. Physik* **1972**, *255*, 146–160.

(20) Jardine, A. P.; Hedgeland, H.; Alexandrowicz, G.; Allison, W.; Ellis, J. Helium-3 Spin-Echo: Principles and Application to Dynamics at Surfaces. *Prog. Surf. Sci.* **2009**, *84*, 323–379.

(21) Van Hove, L. Correlations in Space and Time and Born Approximation Scattering in Systems of Interacting Particles. *Phys. Rev.* **1954**, *95*, 249–262.

(22) Squires, G. *Introduction to the Theory of Thermal Neutron Scattering*; Cambridge University Press: Cambridge, U.K., 1978.

(23) Lechner, B. A. J.; Kole, P. R.; Hedgeland, H.; Jardine, A. P.; Allison, W.; Hinch, B. J.; Ellis, J. Ultra-High Precision Determination of Site Energy Differences using a Bayesian Method. *Phys. Rev. B* **2014**, *89*, 121405.

(24) Chudley, C. T.; Elliot, R. J. Neutron Scattering from a Liquid on a Jump Diffusion Model. *Proc. Phys. Soc.* **1961**, *77*, 353–361.

(25) Jardine, A. P.; Ellis, J.; Allison, W. Effects of Resolution and Friction in the Interpretation of QHAS Measurements. *J. Chem. Phys.* **2004**, *120*, 8724–33.

(26) Hedgeland, H.; Fouquet, P.; Jardine, A. P.; Alexandrowicz, G.; Allison, W.; Ellis, J. Measurement of Single-Molecule Frictional Dissipation in a Prototypical Nanoscale System. *Nature Phys.* **2009**, *5*, 561–564.

(27) Jardine, A. P.; Hedgeland, H.; Ward, D.; Xiaoqing, Y.; Allison, W.; Ellis, J.; Alexandrowicz, G. Probing Molecule-Surface Interactions through Ultra-Fast Adsorbate Dynamics: Propane/Pt(111). *New J. Phys.* **2008**, *10*, 125026.

(28) Hedgeland, H.; Lechner, B. A. J.; Tuddenham, F. E.; Jardine, A. P.; Allison, W.; Ellis, J.; Sacchi, M.; Jenkins, S. J.; Hinch, B. J. Weak Intermolecular Interactions in an Ionically Bound Molecular Adsorbate: Cyclopentadienyl/Cu(111). *Phys. Rev. Lett.* **2011**, *106*, 186101.

(29) Lechner, B. A.; Sacchi, M.; Jardine, A. P.; Hedgeland, H.; Allison, W.; Ellis, J.; Jenkins, S. J.; Dastoor, P. C.; Hinch, B. Jumping, Rotating and Flapping: The Atomic Scale Motion of Thiophene on Cu(111). *J. Phys. Chem. Lett.* **2013**, *4*, 1953–1958.

(30) Guantes, R.; Vega, J. L.; Miret-Artés, S.; Pollak, E. Kramers' Turnover Theory for Diffusion of Na Atoms on a Cu(001) Surface Measured by He Scattering. *J. Chem. Phys.* **2003**, *119*, 2780–2791.

(31) Ianconescu, R.; Pollak, E. A Study of Kramers' Turnover Theory in the Presence of Exponential Memory Friction. *J. Chem. Phys.* **2015**, *143*, 104104.

(32) Shimanouchi, T. *Tables of Molecular Vibrational Frequencies Consolidated Volume I*; National Bureau of Standards: Washington, U.S.A., 1972; pp 1–160.

(33) Clark, S. J.; Segall, M. D.; Pickard, C. J.; Hasnip, P. J.; Probert, M. J.; Refson, K.; Payne, M. First Principles Methods using CASTEP. *Z. Kristallogr.* **2005**, *220*, 567–570.

(34) Ferri, N.; Distasio, R. A.; Ambrosetti, A.; Car, R.; Tkatchenko, A.; Ab, A. B. Electronic Properties of Molecules and Surfaces with a Self-Consistent Interatomic van der Waals Density Functional. **2015**, *176802*, 1–5.

(35) Carrasco, J.; Liu, W.; Michaelides, A.; Tkatchenko, A. Insight into the description of van der Waals forces for benzene adsorption on transition metal (111) surfaces. *Journal of Chemical Physics* **2014**, *140*.

(36) Tkatchenko, A.; DiStasio, R. A.; Car, R.; Scheffler, M. Accurate and Efficient Method for Many-Body van der Waals Interactions. *Phys. Rev. Lett.* **2012**, *108*, 236402.

(37) Ruiz, V. G.; Liu, W.; Zojer, E.; Scheffler, M.; Tkatchenko, A. Density-Functional Theory with Screened van der Waals Interactions for the Modeling of Hybrid Inorganic-Organic Systems. *Phys. Rev. Lett.* **2012**, *108*, 146103.

(38) Meehan, P.; Rayment, T.; Thomas, R. K.; Bomchil, G.; White, J. W. Neutron Diffraction from Benzene Adsorbed on Graphite. *J. Chem. Soc., Faraday Trans. 1* **1980**, *76*, 2011–2016.

(39) Tkatchenko, A.; Scheffler, M. Accurate Molecular Van Der Waals Interactions from Ground-State Electron Density and Free-Atom Reference Data. *Phys. Rev. Lett.* **2009**, *102*, 073005.

(40) Grimme, S. Semiempirical GGA-Type Density Functional Constructed with a Long-Range Dispersion Correction. *J. Comput. Chem.* **2006**, *27*, 1787–1799.

(41) Sacchi, M.; Jenkins, S.; Hedgeland, H.; Jardine, A. P.; Hinch, B. J. Electronic Structure and Bonding of an Ionic Molecular Adsorbate: c-C_5H_5 on Cu(111). *J. Phys. Chem. B* **2011**, *115*, 16134–16141.